ADVANCED FUNCTIONAL MATERIALS

www.afm-journal.de

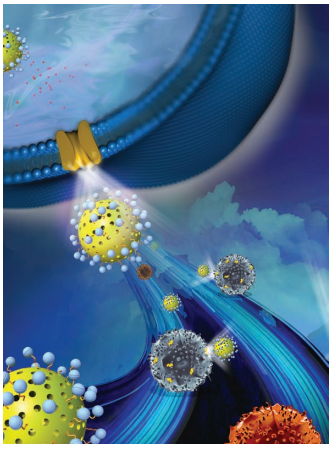

Drug Delivery

In this study, T. Chen and co-workers present a cancer-targeted MSN drug-delivery system carrying ruthenium complexes (RuPOP@MSNs), that allows the direct fluorescence monitoring of the cellular uptake and localization of theranostic agents in cancer cells. On page 2754 the nanoparticles exhibit unprecedented enhanced cytotoxicity toward cancer cells overexpressing integrin receptors through the induction of apoptosis. Moreover, the strong autofluorescence of Ru complex extends the power of theranostics to a subcellular level.

Graphene

Reduced graphene oxide (rGO) films are decorated with arrays of Au nanoparticles using diblock copolymer micelles by T. D. Chung, B.-H. Sohn, and co-workers. On page 2764, they show how decorated rGO films can be transferred to various substrates including carbon electrodes and flexible polymer films without deterioration of the arrays. Decorated rGO films show high electrochemical activity for the oxygen reduction reaction (ORR), and a size-dependent ORR mechanism is analyzed electrochemically based on a rotating disk electrode.

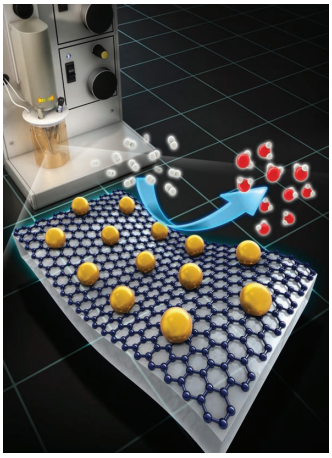

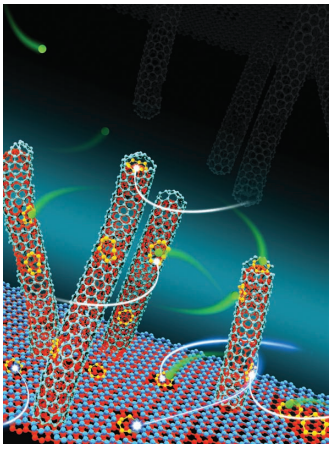

Carbon

The rational hybridization of sp2 nanocarbon and nanostructured porous carbon into hierarchical all-carbon nanoarchitectures which inherit all the advantages of the component materials is demonstrated by Q. Zhang, F. Wei, and co-workers on page 2772. The sp2 graphene/CNT interlinked networks result in superior electrical conductivity and a robust framework, while the meso-/microporous carbon and the interlamellar compartment before the opposite graphene accommodate sulfur and polysulfides for lithium-sulfur cells with large sulfur loading, high discharge capacity, and stable cycling performance.

CONTENTS

FULL PAPERS

Emission

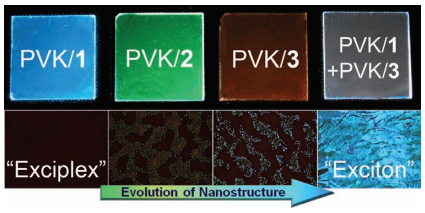

Color-tunable exciplex emission based on a polymeric donor (PVK) and nanostructured acceptors is studied, including its ability to switch to exciton emission. Color-tunable exciplexes are obtained by incorporating highly fluorescent acceptors with different molecular energy levels. Emission switching depending on the evolution of nanostructures at the donor–acceptor interface is investigated, taking advantage of self-assembly of the supramolecular acceptors.

Drug Delivery

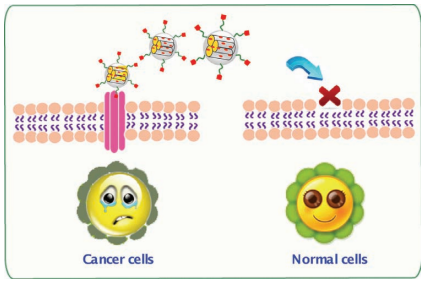

Cancer-targeted MSNs loaded with a novel Ru polypyridyl complex (RuPOP@MSNs) that allows the direct fluorescence monitoring of the cellular uptake and localization of anticancer agents in cancer cells are presented. The internalized RuPOP@MSNs can control the release of free Ru complex to trigger ROS-mediated p53 phosphorylation and to regulate the AKT and MAPKs signaling pathways.

Graphene

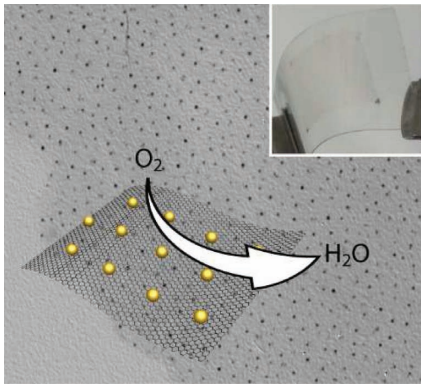

Reduced graphene oxide (rGO) films are decorated with non-overlapping Au nanoparticles using diblock copolymer micelles that provide controllability over the number density as well as the diameter of the nanoparticles. The rGO film enables the transferability of the Au nanoparticles without deterioration of their arrays, which exhibit high electrochemical activity in the oxygen reduction reaction.

Carbon

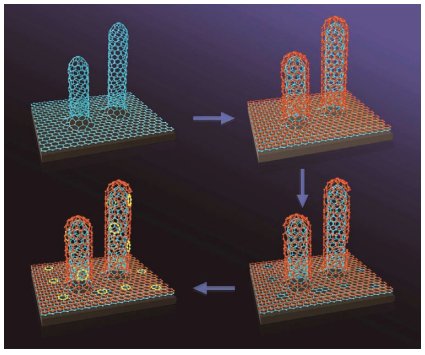

3D interconnected graphene/CNT networks are coated with porous carbon. The sp^2 graphene/CNT interlinked network gives the composites good electrical conductivity and a robust framework, while the meso-/microporous carbon and the interlamellar compartment between the opposite graphene accommodate sulfur and polysulfides, provide accessibility for liquid electrolyte to active materials, and restrain the shuttle phenomenon.

FULL PAPERS

Three classes of p- and n-type conjugated polymers with different functional groups are designed and synthesized with electron neutral thienyl-vinylene (TVTOEt) and electron rich or electron deficient building blocks. The different functional groups influence the polymer electronic energy levels, thin film morphologies, and charge transfer properties. The all-polymer photovoltaic devices using the n-type copolymer as the acceptor material exhibit good efficiency.

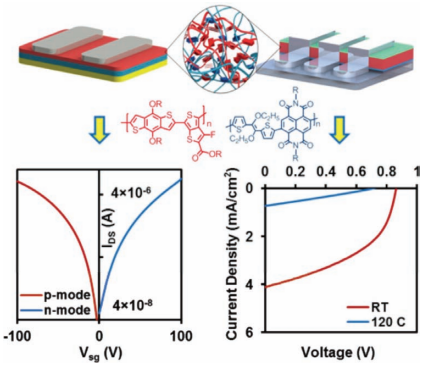

Conjugated Polymers

A new Schottky junction near-infrared light photodetector is fabricated by coating a GaAs nanocone array with a monolayer graphene film, which shows high sensitivity to near-infrared light irradiation, with good reproducibility, excellent selectivity, and rapid response speed.

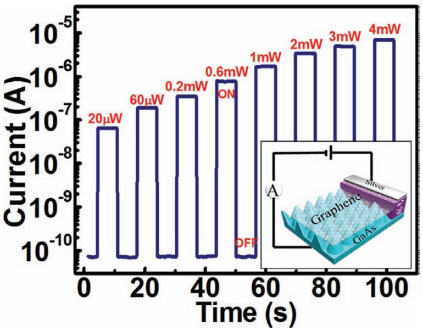

Photodetectors

A novel UV-induced fabrication of nano/macro hierarchical structures of triblock copolymer lamellar films is developed. The method is based on a change in the water affinity of the films activated by UV light. Osmotic pressure at the interface between illuminated and unilluminated parts drives the molecular migration for surface pattern formation. This remarkable advantage makes this method exceptionally versatile.

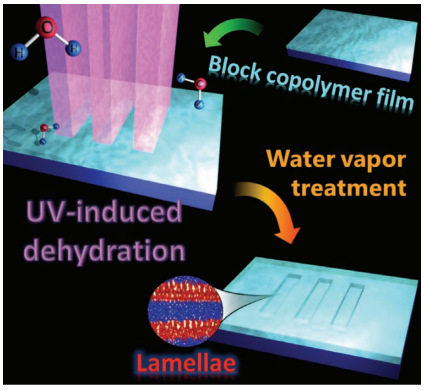

Micropatterns

A fully integrated and active UV photodetector based on a triboelectric nanogenerator configuration is successfully demonstrated. Dendritic TiO_2 nanostructures are designed as a built-in photodetector and contact material of the triboelectric nanogenerator. With the advantages of easy fabrication, low cost, rapid response time, and excellent responsivity, this self-powered active UV photodetector presents a new approach for building functional devices.

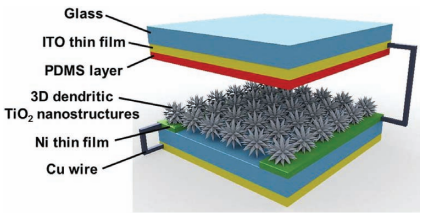

Photodetectors

CONTENTS

FULL PAPERS

Cancer Treatment

Photothermal Killing of Cancer Cells by the Controlled Plasmonic Coupling of Silica-Coated Au/Fe_2O_3 Nanoaggregates

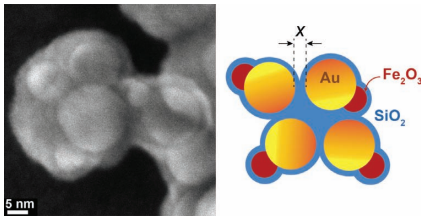

Twin or Janus-like gold-iron-oxide plasmonic-superparamagnetic nanoaggregates are made by flame aerosol technology and wrapped up "in-flight" by a transparent silica nanothin film. Its thickness finely tunes the near-infrared absorption of Au nanoparticles allowing for a high light-to-heat efficiency, while iron-oxide facilitates their magnetic placement and in-vivo monitoring by MRI, and killing human breast cancer cells with a short, 4-minute laser irradiation.

Metal Nanostructures

Highly Asymmetric, Interfaced Dimers Made of Au Nanoparticles and Bimetallic Nanoshells: Synthesis and Photo-Enhanced Catalysis

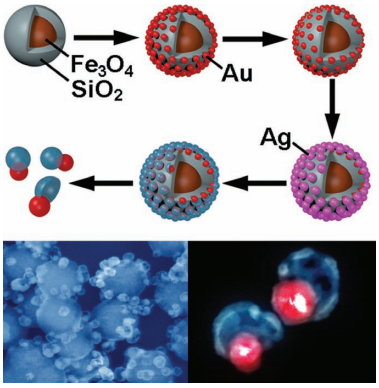

Highly asymmetric, interfaced dimers made of solid Au nanoparticles and hollow bimetallic nanoshells with different compositions are synthesized by combining the controlled growth of interfaced Au–Ag dimers and nanoscale galvanic replacement reactions on superparamagnetic colloidal substrates. The direct contact between the Au nanoparticle and the bimetallic nanoshells leads to possible strong couplings and novel properties.

Ionic Liquids

DyeIonogels: Proton-Responsive Ionogels Based on a Dye-Ionic Liquid Exhibiting Reversible Color Change

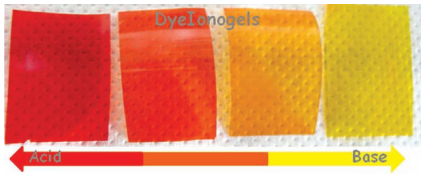

The combination of the ionic liquid (IL) 1-butyl-3-methylimidazolium bis(trifluoromethane sulfonyl)imide, a dye-IL (DIL, 1-butyl-3-methylimidazolium methyl orange), and poly(methylmethacrylate) (PMMA) yields transparent, ion-conducting, and flexible ionogels with a strong and reversible color change when acidic or basic environments. The ionogels are prototypes of soft multifunctional matter featuring a strong readout signal, the color change, that could be used in optical data storage or environmental sensing.

Ferroelectrics

Interesting Evidence for Template-Induced Ferroelectric Behavior in Ultra-Thin Titanium Dioxide Films Grown on (110) Neodymium Gallium Oxide Substrates

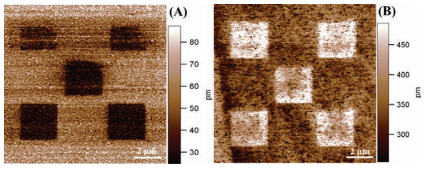

Interesting evidence is presented for ferroelectric behavior in ultra-thin, highly-strained epi-films of anatase-TiO_2 on (110) $NdGaO_3$ substrates grown by CVD. The evidence includes: a bipolar domain structure, bipolar polarization switching in PFM, excellent polarization stability with time/temperature, and a Curie point between 180 and 200 °C. A Slater model is presented for ferroelectricity in this technologically-important material.

FULL PAPERS

Silicon doped with sulfur to supersaturated concentrations exhibits strong sub-band gap extrinsic absorption from a dopant induced impurity band. By tuning the Fermi level using dopant compensation, it is possible to tailor the infrared photoresponse, demonstrating, for the first time, room-temperature extrinsic photoconductivity in this material using photon energies below the silicon band gap.

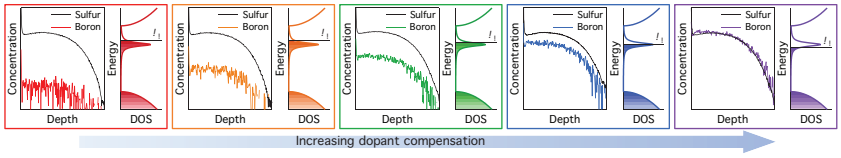

Supporting single-site catalysts on electrospun polyvinyl alcohol (PVA) nanofiber nonwovens enables the in-situ formation of structured ultrahigh molecular weight polyethylene (UHMWPE) nanofibers during polymerization. Herein a new generation of shape-replication catalysts producing nanoporous polyolefins, useful as solvent-resistant filters, is investigated.

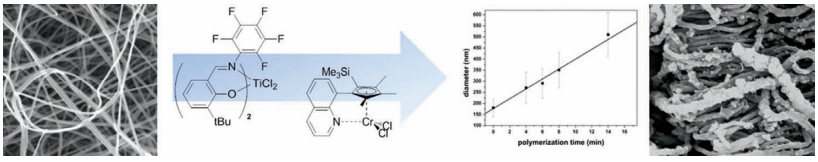

Model chemical vapor deposition (CVD) and mechanically exfoliated graphene coatings are demonstrated as wide area strain sensors by following Raman band shifts over cyclic deformation sequences. CVD coatings with calculated absolute accuracy of ≈0.01% strain and resolution of ≈27 microstrains would be a viable candidate for practical applications.

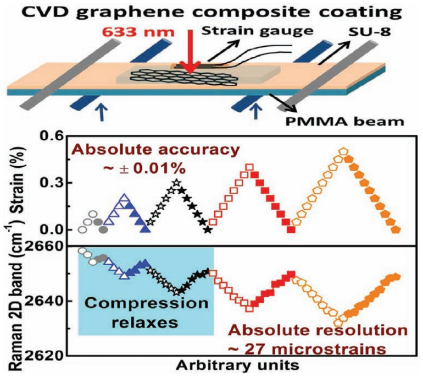

For Ga-doped ZnMgO, addition of Mg to ZnO increases the band gap but also results in an increased number of dopant (Ga_{Zn}) compensating zinc vacancies (V_{Zn}). Post-deposition annealing induces Ga_{Zn}-V_{Zn} defect clustering which improves the electron mobility by reducing the net ionized impurity scattering.

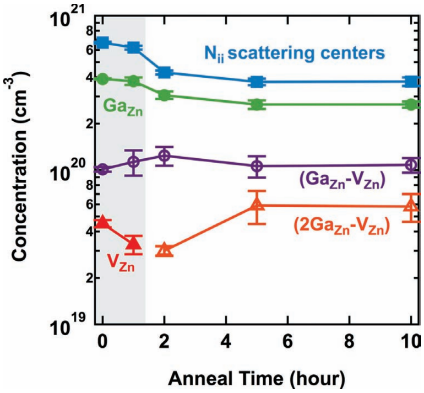

CONTENTS

FULL PAPERS

Composite Films

Defect-Tolerant Nanocomposites through Bio-Inspired Stiffness Modulation

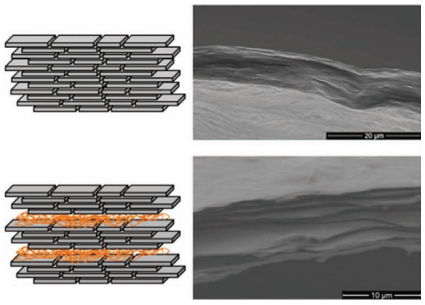

Graphene oxide-PMMA composite films with a multilayer laminate structure are shown to have greatly enhanced mechanical stiffness and strength compared to pure-graphene-oxide films. The thin polymer layers impart crack-deflection and stopping mechanisms that prevent catastrophic failure upon local failure and crack propagation, thereby making the material less sensitive to defects.

Nanogenerators

Increase Output Energy and Operation Frequency of a Triboelectric Nanogenerator by Two Grounded Electrodes Approach

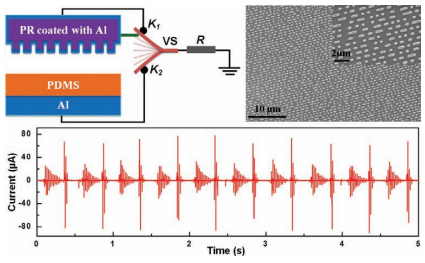

The two-electrodes-grounded triboelectric nanogenerator (TEG-TENG) is developed. The TEG-TENG can double the generated charges and enhance the output frequency compared to the traditional non-grounded TENG. The output energy at a load lower than 10 MΩ is also enhanced, and the enhanced ratio is more than 100 at a load of 100 kΩ.

Intracellular Delivery

A DNA Device that Mediates Selective Endosomal Escape and Intracellular Delivery of Drugs and Biologicals

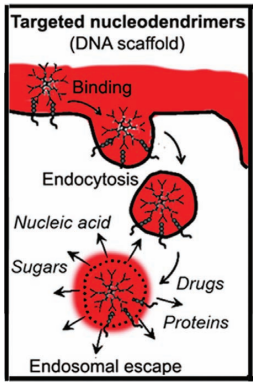

DNA devices enter cells and provide cytosolic delivery. However, specificity of targeting and uptake via selected routes, as well as potential to deliver a broad spectrum of compounds intracellularly, has not been demonstrated. Using model 200 nm DNA dendrimers (nucleodendrimers), compared to control polymer nanoparticles, this work describes that both, high specificity and a wide range of applications can be achieved.

Organic Semiconductors

Molecular Packing-Induced Transition between Ambipolar and Unipolar Behavior in Dithiophene-4,9-dione-Containing Organic Semiconductors

Organic semiconductor materials with the same conjugated core can exhibit either unipolar or ambipolar transport behavior in thin-film transistors. Experimental and theoretical investigations reveal that the drastic differences in transport properties are due to their different molecular packing and thin-film structures induced by the different alkyl substitutes.